SCIENCE CHINA
Information Sciences

• LETTER •

August 2025, Vol. 68, Iss. 8, 189401:1–189401:2
https://doi.org/10.1007/s11432-024-4361-4

Potential of boron nitride/diamond heterostructures for *n*- and *p*-type conduction

Yao LI[1], Chenxu WANG[1], Qun LI[1*], Jinfeng ZHANG[2], Kai SU[2], Jichao HU[1], Tao LIN[1], Zeyang REN[2], Jiaduo ZHU[2], Yachao ZHANG[2] & Yue HAO[2]

[1]*Department of Electronic Engineering, Xi'an University of Technology, Xi'an 710048, China*
[2]*State Key Discipline Laboratory of Wide Band Gap Semiconductor Technology, School of Microelectronics, Xidian University, Xi'an 710071, China*

Received 13 December 2024/Revised 28 February 2025/Accepted 24 March 2025/Published online 1 July 2025

Citation Li Y, Wang C X, Li Q, et al. Potential of boron nitride/diamond heterostructures for *n*- and *p*-type conduction. Sci China Inf Sci, 2025, 68(8): 189401, https://doi.org/10.1007/s11432-024-4361-4

Given the advantages of diamond in terms of carrier mobility, thermal conductivity, breakdown voltage, and chemical stability, it offers great potential in high-temperature and high-power electronic fields. However, the activation of dopants is relatively hard for both donor and acceptor types. Hexagonal boron nitride (h-BN) and cubic zinc-blende (c-BN) structures have attracted great attention because of their structures and properties similar to those of graphite and diamond. In particular, h-BN, a two-dimensional (2D) insulator with low dielectric constant and excellent chemical and thermal stability, is deemed a promising gate dielectric for diamond field-effect transistors (FETs). Using an air-free process, hole mobility in hydrogen-terminated diamond FETs with an h-BN gate dielectric was previously increased to 680 cm^2/Vs [1]. Furthermore, a large valence band offset (2.08 eV) of the h-BN/diamond heterostructure was determined using Kraut's method, favoring the accumulation of a high hole density at the heterointerface [2]. Despite the obstacles in growing pure cubic and single crystal BN materials, great effort has been devoted theoretically and experimentally to promoting the application of c-BN in diamond channel-based electronic devices. For instance, Shammas et al. [3] reported a type-II alignment of c-BN/diamond heterostructures, and the conduction band offset was determined as 1.7 eV using X-ray photoelectron spectroscopy measurement. In this work, 2D electron gas with a high density of $\sim 10^{13}$ cm^{-2} was assumed to be possible in c-BN/diamond heterostructures. Furthermore, the *n*-type or *p*-type surface doping appearing at c-BN/diamond heterostructures can be modulated by interface C–N or C–B bond configuration, resulting in a high areal electron or hole density of 10^{13}∼10^{14} cm^{-2}. To conclude, BN/diamond heterostructures, whether hexagonal or cubic, are promising candidates for high-performance electronic devices with superior electronic transport properties of 2D carriers.

The electron transport properties in c-BN/diamond heterostructures were studied previously [4]. However, analyses of *p*-type conduction in BN/diamond heterostructures are lacking. In this study, we systematically investigate the variation of hole density with the Schottky barrier height, barrier layer thickness, and modulation doping (MD) density. We model the hole mobility considering the conventional five scattering mechanisms and study its variation with barrier layer thickness and temperature. The effect of variation parameters in wavefunction on mobility is also investigated, and *n*- and *p*-type conduction are compared in BN/diamond heterostructures.

According to Chen et al. [2], a type-II band alignment with a valence band offset of 2.08 eV is assumed for the BN/diamond heterostructure. Figures 1(a) and (b) show the schematic structure and the relevant band diagram of the BN/diamond heterostructure, respectively. Here, t_b and t_i are the thicknesses of the barrier layer and the undoped spacer layer, respectively. Following the model by Delagebeaudeuf et al. [5], the hole density in the BN/diamond heterostructure is calculated, whose formula is listed as Eq. (1) in Appendix A.

Besides the band offset, there are uncertainties in the Schottky barrier height Φ_b of the BN/diamond heterostructure, which ranges from 0.5 to 4.8 eV. Here, the upper limit is obtained by presuming Au as the Schottky metal and subtracting the experimental electron affinity of BN (0.3 eV). In the calculation, the 2D hole gas (2DHG) is neglected if its density is lower than 10^{10} cm^{-2}. Figure S1 in Appendix B proves that the existence of 2DHG is only possible when $\Phi_b < 3.58$ eV when the barrier is undoped. The 2DHG density p_s in the uniformly doped barrier layer shows an initially descending and then rising curve for small Φ_b (Figure S2 in Appendix B). For larger Φ_b, p_s first rises sharply and then saturates with barrier layer thickness.

Figures 1(c) and (d) illustrate the relation of p_s with the barrier layer thickness and MD density N_A for different Schottky barrier heights. As the increase of N_A in the barrier layer means more 2DHG in the heterointerface, the

* Corresponding author (email: liqun@xaut.edu.cn)

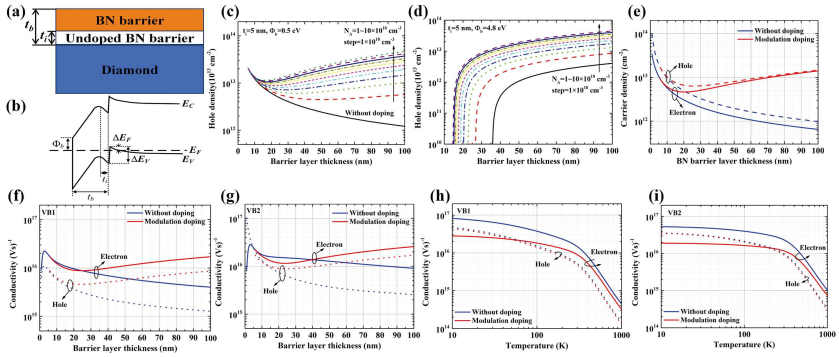

Figure 1 (Color online) (a) Schematic of a BN/diamond heterostructure; (b) energy band diagram of a *p*-type modulation doped BN/diamond heterostructure; dependence of the hole density on the thickness of the BN barrier layer considering the MD for different Schottky barrier heights: (c) 0.5 eV and (d) 4.8 eV; (e) comparison of electron and hole density as functions of the BN barrier layer thickness for the cases without doping and with MD; comparison of *n*- and *p*-type conductivities as functions of the BN barrier layer thickness for the cases without doping and with MD for different variation parameters: (f) VB1 and (g) VB2; comparison of *n*- and *p*-type conductivities as functions of temperature for the cases without doping and with MD for different variation parameters: (h) VB1 and (i) VB2.

special barrier layer thickness for the minimum p_s point at low Φ_b (< 3.58 eV) decreases accordingly, the same as the critical barrier layer thickness for the 2DHG at high Φ_b, which reduces from 36 to 15 nm when N_A increases from 1×10^{18} to 10×10^{18} cm^{-3}.

Figure 1(e) compares the electron and hole density in BN/diamond heterostructures with undoped and MD barrier layers. Apparently, the hole density is larger or comparable to the electron density in the considered range of barrier layer thickness. MD becomes effective only when the barrier layer is thicker than 10 nm. The hole and electron density curves converge to similar values when the MD barrier layer is thick enough. For the undoped barrier layer, the variation of the hole density with the barrier layer thickness is almost parallel to the electron counterpart.

Then, contrasts are made for electron/hole mobility considering the difference in the variational parameter b. That is, in our previous study of diamond *p*-type channel [6], b adopted as $\left[33\pi m_d^* e^2 p_s/2\hbar^2\varepsilon_0\varepsilon_s\right]^{1/3}$ was conducive to the fitting of theoretical mobility with the experimental data. Meanwhile, for other 2D carrier studies [7], the parameter b is also taken as $\left[33m_d^* e^2 p_s/8\hbar^2\varepsilon_0\varepsilon_s\right]^{1/3}$. The case using the former b is defined as VB1, whereas the latter counterpart is marked as VB2. The hole mobility is calculated considering the conventional interface roughness, acoustic phonon (AC), nonpolar optical phonon (NOP), MD, and remote surface roughness (RSR) scattering, whose formulas are shown as Eqs. (2)–(7) in Appendix C. Here, the default value of Φ_b is 1.1 eV, N_A is 3×10^{18} cm^{-3}, and t_i is 5 nm.

We illustrate the detailed hole mobility curves in Figures S3–S6 in Appendix D, and contrasts of the electron and hole mobility are made in Figures S7 and S8 in Appendix E. The electron counterparts are similar to those in [4]. Figures 1(f)–(i) show the *n*-/*p*-type conductivity, represented by the product of electron/hole density and mobility, as functions of barrier layer thickness and temperature. For VB1, the maximum conductivities lie at the barrier layer of ∼3 nm for the electron and ∼2 nm for the hole if the barrier is undoped. Meanwhile, for the MD barrier, the minimum conductivities are at the barrier layer of ∼25 nm for the electron and hole. For VB2, the location of the peak conductivity for the electron in undoped heterostructures is still ∼3 nm, whereas the *p*-type conductivity monotonously decreases with the barrier layer thickness. For the MD barrier, the minimum conductivities manifest at the barrier layer of ∼24 and 25 nm for the electron and hole. In VB1, the *n*-type conductivity is generally larger than the p-type conductivity, except when the barrier is over 54 nm and undoped. In VB2, a similar case occurs when the barrier is over 60 nm and undoped. Furthermore, with the barrier layer undoped and thinner than 4 nm, the *p*-type conductivity in VB2 can be larger than the *n*-type conductivity in both cases. In Figures 1(h)–(i), the carrier densities are independent of temperature and taken as 4.6×10^{12} and 6.6×10^{12} cm^{-2} for the electron and hole, respectively. Therefore, the conductivity curves are similar to their mobility counterparts (see Figure S8 in Appendix E). The *p*-type conductivity for VB1 can be larger than the *n*-type conductivity with the MD barrier layer when the temperature is lower than ∼55 K, whereas the critical temperature for VB2 rises to 200 K.

Acknowledgements This work was supported by National Natural Science Foundation of China (Grant Nos. 62404180, 62474139, 62171367) and Major Projects of Shanxi Province (Grant Nos. 20201102012, 202202030201001).

Supporting information Appendixes A–E. The supporting information is available online at info.scichina.com and link.springer.com. The supporting materials are published as submitted, without typesetting or editing. The responsibility for scientific accuracy and content remains entirely with the authors.

References

1 Sasama Y, Kageura T, Imura M, et al. High-mobility p-channel wide-bandgap transistors based on hydrogen-terminated diamond/hexagonal boron nitride heterostructures. Nat Electron, 2021, 5: 37–44
2 Chen J, Tao R, Wang G, et al. The interface microstructure and band alignment of hexagonal boron nitride/diamond heterojunctions. J Mater Chem C, 2023, 11: 5324–5330
3 Shammas J, Yang Y, Wang X, et al. Band offsets of epitaxial cubic boron nitride deposited on polycrystalline diamond via plasma-enhanced chemical vapor deposition. Appl Phys Lett, 2017, 111: 171604
4 Li Y, Zhang J, Wang Y, et al. Predicted mobility of 2-D electrons in c-BN/diamond heterostructures. IEEE Trans Electron Devices, 2024, 71: 5824–5830
5 Delagebeaudeuf D, Linh N T. Metal-(n) AlGaAs-GaAs two-dimensional electron gas FET. IEEE Trans Electron Devices, 1982, 29: 955–960
6 Li Y, Zhang J F, Liu G P, et al. Mobility of two-dimensional hole gas in H-terminated diamond. Phys Rapid Res Ltrs, 2018, 12: 1700401
7 Ridley B K, Foutz B E, Eastman L F. Mobility of electrons in bulk GaN and $Al_xGa_{1-x}N$/GaN heterostructures. Phys Rev B, 2000, 61: 16862–16869